

Influence of high density particles in reduction of axial dispersion in liquid fluidized bed with residence time distribution curve studies

Jamshid Behin[†] and Tahereh Shojaeimehr

Department of Chemical Engineering, Faculty of Engineering, Razi University, Kermanshah, Iran
(Received 6 September 2010 • accepted 8 October 2010)

Abstract—Liquid phase RTD curves were investigated in classical fixed and fluidized bed regimes with high density particles. The effect of liquid velocity was studied on bed hydrodynamics. Using an impulse tracer injection technique in a column of 5 cm inner diameter and 1.2 m height, liquid RTD, mean residence time (MRT), axial dispersion coefficient (ADC) and vessel dispersion number (N_D) were determined. ADC increases with liquid superficial velocity. It varied from 4.63 to 20.7 cm²/s for the particle Reynolds number of 43 to 279, respectively. The experimental results show that the high density particles cause less ADC than the low density particles at an identical Reynolds number.

Key words: Axial Dispersion Coefficient, Hydrodynamics, Liquid-solid Fluidized Bed, Residence Time Distribution

INTRODUCTION

Liquid-solid fixed and fluidized beds are encountered in many processes in industrial operations. Numerous examples can be found in the chemical, petrochemical, pharmaceutical, agricultural, biochemical, hydrometallurgical, electrical power-generation, and food industries. Water treatment, catalytic cracking, combustion, crystallization, ion exchange, and adsorption are examples of liquid-solid fluidized beds [1-4]. Because of the low efficiency of the conventional fixed bed system, much attention has been paid to fluidized bed systems. These are common and important reactors in process engineering because of easy handling, good mixing and transportation, good mass-heat transfer rates between the fluid and the particles and also between the particles and the sidewall [5]. The efficient-successful design, analysis, operation, scale-up, optimization, and prediction of the hydrodynamic behavior of these beds require detailed knowledge of axial dispersion coefficient (ADC) [3,6]. It provides information about the degree of fluid mixing existing in the bed. Axial liquid phase mixing is a key factor that greatly affects the interphase heat and mass transfer rates, the reactant concentration distribution, and ultimately reactant conversions [7,8]. Residence time distribution (RTD) studies have proved indispensable in the understanding of hydrodynamics of fluidized beds, where a tracer is injected at some locations of the bed and its concentration is monitored at a point in downstream. The tracer concentration distribution data is processed to extract quantitative information about the dispersion characteristics of the bed [7]. Among the studies on ADC in liquid-solid fluidized beds, the most extensive work was reported by Chung and Wen [9], who proposed a generalized correlation for ADC in both fixed and fluidized beds. Kikuchi et al. [10] reported that ADC in a fluidized bed of polystyrene particles deviated significantly from literature correlation equations, including that obtained by Chung and Wen. Tang and Fan [8] measured ADC of low density particles (polystyrene, acrylic, nylon, etc.) in liquid-solid

fluidized beds. They used a column of 7.6 cm inner diameter and 130 cm height. The particles had densities and diameters ranging 1.05-1.3 g/cm³ and 1-2.5 mm, respectively. They analyzed dispersion of tracer based on the axial dispersion model and showed that a liquid's ADC is proportional to the liquid superficial velocity to a power of 1.28 for low density particles. To compare the axial liquid mixing behavior's results in beds of low density particles with most of the literature data for heavy particles, an experimental run for a fluidized bed of heavy particles, 1.0 mm glass beads, was performed by Tang and Fan [8]. They obtained an axial dispersion coefficient of 7.64 cm²/s in the 1.0 mm glass beads at the superficial liquid velocity of 5.0 cm/s and a bed void fraction of 0.634, which compared to 8.06 cm²/s calculated from the Chung and Wen correlation equation. Their results indicate that the difference, if one exists, between the axial liquid mixing behavior in beds of low density particles and that reported in the literature for beds of heavy particles cannot be attributed to the measuring method applied and the column and distributor design used in their study. They also studied the relationship between ADC and the bed void fraction. The ADC for all the low density particles increases monotonically with increasing bed void fraction. It appears that for the same bed void fraction, particles with higher terminal velocity have higher value of ADC. The results are expected since a higher relative liquid velocity is required to maintain a given bed void fraction for particles with a higher terminal velocity. Consequently, higher turbulence will be generated, which in turn leads to higher extent of mixing. Asif et al. [7] studied the effect of liquid velocity on the ADC with negligible distributor effect. The fluidized bed was a column of 7.68 cm in diameter. They determined ADC of 2-12 cm²/s for cylindrical propylene particles (ρ_p : 1.61 g/cm³, d_p : 3.0 mm, L_p : 3.0 mm, U_o : 2-10 cm/s), 4-35 cm²/s for spherical glass particles (ρ_p : 2.46 g/cm³, d_p : 2.0-3.0 mm, U_o : 4-16 cm/s), respectively. Liquid phase residence time distribution studies are reported in 2-phase inverse fluidized bed for the first time by Renganathan and Krishnaiah [6]. They studied the mixing characteristics of the liquid phase in liquid-solid inverse fluidized bed for very low density particles of 0.897 g/cm³. They showed that the liquid phase ADC increases with increase in liquid

[†]To whom correspondence should be addressed.
E-mail: Behin@razi.ac.ir

velocity and is independent of static bed height. The liquid phase ADC is reported to increase with increase in liquid velocity and reach a maximum at a velocity corresponding to a void fraction around 0.7 and decrease with further increase in liquid velocity. However, also observed by Chung and Wen [9] and Tang and Fan [11] was a monotonic increase of dispersion coefficient with increase in liquid velocity even beyond a void fraction of 0.7 [6].

In the present investigation, experiments were performed in the three different tests: one in the column filled with only liquid phase without solid particles, and two tests in the fixed and fluidized bed regimes, respectively. The aim of this work was to study the liquid phase RTD curves, and the effect of liquid velocity on hydrodynamics of bed for heavy particles using an impulse tracer injection technique.

1. Axial Dispersion Model

The concentration distribution in the fluid phase of a liquid fluidized bed containing inert, nonadsorbing component and nonporous solid is given by the following dispersion equation:

$$\frac{\partial C}{\partial t} = D_1 \frac{\partial^2 C}{\partial x^2} - U_{act} \frac{\partial C}{\partial x} \quad (1)$$

Where D_1 is the axial dispersion coefficient describing the degree of dispersion (by diffusion and liquid mixing) in the direction of flow (x) through the column and U_{act} is the liquid interstitial (actual) velocity ($U_{act} = U_o / \varepsilon$) in which U_o and ε are liquid superficial velocity and average void fraction of bed, respectively. This equation can be written in dimensionless form [12]:

$$\frac{\partial C}{\partial \theta} = \left(\frac{D_1}{U_{act} L} \right) \frac{\partial^2 C}{\partial z^2} - \frac{\partial C}{\partial z} \quad (2)$$

with

$$z = \frac{x}{L} \quad (3)$$

and dimensionless time:

$$\theta = \frac{t \cdot U_{act}}{L} \quad (4)$$

L is the height of bed. Therefore, the RTD of the system (E-curve) can be obtained from the following equation [13]:

$$E_\theta = \frac{1}{2} \left(\frac{Pe}{\pi \theta} \right)^{1/2} \cdot \exp \left(- \frac{Pe}{4} \cdot \frac{(1-\theta)^2}{\theta} \right) \quad (5)$$

with mass Peclet number:

$$Pe = \frac{U_o \cdot L}{\varepsilon \cdot D_1} \quad (6)$$

The dispersion model uses a single parameter to describe mixing, which is termed the vessel dispersion number (approximately inverse of mass Peclet number):

$$N_D = \frac{D_1}{U_{act} \cdot L} \quad (7)$$

The vessel dispersion number relates convective transport of liquid to dispersion and is used to describe the influence of axial mixing on the performance of the whole fluidized bed setup. If there is a large deviation from plug flow (i.e., $N_D > 0.01$), the tracer response

is broad and spreads as it slowly passes the measurement point giving an asymmetric response; the assumptions made in the use of short-cut method are no longer valid [12].

The measurement and analysis of RTD are important tools to study the complex phenomena taking place inside the process system. The principle of a tracer experiment consists of a common impulse-response method: injection of a tracer at the inlet of a system and recording the concentration-time curve at the outlet. The interpretation of experimental RTD data has been limited to extracting the mean residence time [12].

EXPERIMENTAL

Experiments were carried out in a classical liquid-solid fluidized bed of 5 cm inner diameter and height of 1.2 m with tap water as the liquid phase and heavy metallic shots as the solid particles (Fig. 1). The density and volume-surface mean diameter of the particles were 10.73 g/cm³ and 2.45 mm, respectively. A plastic mesh was placed at the bottom of the bed as a distributor. The water temperature was 20 °C and its flow rate was kept approximately constant during each run of experiments. The water flow rate was varied from 33-220 cm³/s. Impulse input function method was used to measure the RTD of liquid phase. A 1 cm³ of saturated sodium chloride solution was injected using a syringe through the septum at the bottom of the column as the tracer. The injection point was about 5 cm away from the distributor, so that the response was free from any kind of flow non-uniformities existing in the distributor region and reflected only the effect of the liquid-solid interaction in the bed itself. The time taken for the tracer injection in all the experiments was less than half of a second and considered as nearly impulse. Experiments were designed in such a way that the distance between the tracer injec-

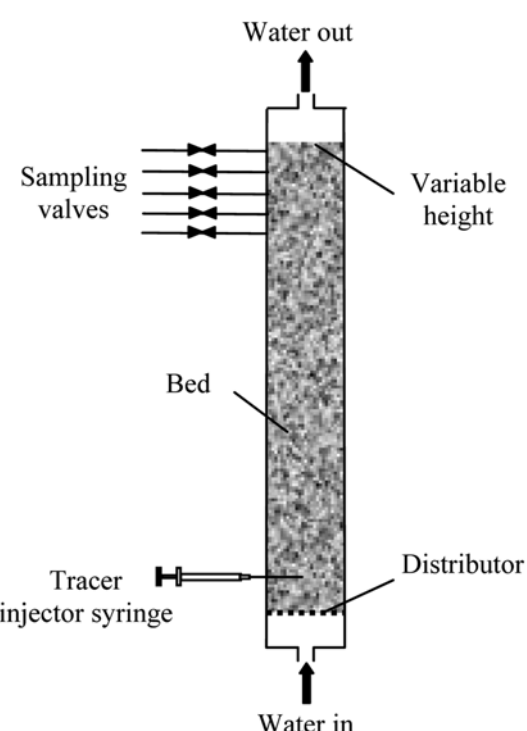


Fig. 1. Schematic diagram of experimental bed.

tion and the tracer sampling points was the same for different tests. For this reason, the liquid was sampled at the top of column by five sampling valves located at different heights. The location of the tracer detection point was always at least 5 cm below the top of the fluidized bed to keep the measurement free from boundary effect. The conductivity of liquid samples was determined by a conductivity meter (Jenway; England) which is an indication of tracer concentration. The bed pressure drop was determined by manometer. Three different tests were run: one in the column filled with only liquid phase without solid phase, and two tests in the fixed and fluidized bed regimes. The values of the bed void fraction were determined from the measured height of the expanded bed.

RESULTS AND DISCUSSION

A great deal of work has been done to characterize the different flow regimes encountered in fluidization. For the small density differences associated with liquid fluidized beds, the bed appears to expand smoothly in what is called uniform (segregate) fluidization. When the density difference between the two phases is large the bed tends to separate into two phases distinguished by their void fraction. There is a dilute bubble phase that consists primarily of fluid with a small number of solid particles suspended in bubbles of fluid and a dense emulsion phase that is primarily solids in composition, what is called bubbling (aggregate) fluidization [14]. Our experimental regime of fluidization is aggregate because of the high difference between liquid and solid densities.

1. Effect of Liquid Velocity on Pressure Drop

Pressure drop of the empty bed was calculated from Darcy-Weisbach equation [15]. Pressure drop in fixed beds was calculated from Foscolo et al. equation. The pressure drop in liquid fluidization is equal to the specific buoyant weight of bed [16]:

$$\frac{\Delta P}{L} = (1 - \varepsilon)(\rho_p - \rho_l)g \quad (8)$$

For the liquid superficial velocity ranging from 1.73 to 11.21 cm/s, the pressure drop of the empty bed varied from 0.00096 to 0.0014 cmHg, which is negligible in comparison with the pressure drop of fixed and fluidized beds. Table 1 shows the effect of liquid flow rate on the pressure drop in fixed and fluidized bed regimes. It increases with increasing liquid flow rate in the two regimes [17,18]. The comparison of the experimentally measured fluidized bed pressure drop was in agreement with the calculated values by the Foscolo et al.

equation [14,17]. The bed voidage increases with increasing liquid flow rate (Reynolds number) which was also observed by Lee [4] and Richardson and Zaki [19].

Fig. 2 shows the effect of liquid flow rate on the RTD of liquid phase in the bed. Fig. 2(a) for an empty bed, Fig. 2(b) for a fixed bed and Fig. 2(c) for a fluidized bed. The variance of RTD curves and liquid MRT decreases with increasing liquid flow rate. The bed started to become fluidized at about 110 cm³/s liquid flow rate, and particle entrainment occurred when the liquid flow rate became more than 220 cm³/s. The results show that the variance of obtained RTD decreases with increasing the liquid flow rate. In addition, with increasing the liquid flow rate (liquid velocity), liquid MRT decreases, and apparently it seems that the mixing regime of liquid became nearly plug flow. The variance of the obtained curves for empty bed is more than those for a fixed bed, and the variance of obtained curves for fixed bed is more than those for a fluidized bed that was also found by Cho et al. [20].

A good understanding of the process can be obtained by simulation of the experimental RTD using models derived from known flow profiles. The parameter of the model, i.e., axial dispersion coefficient (D_a), was obtained by minimizing the residual sum of squares of the deviation between the experimental E-curve and that predicted by model, i.e., the sum of squares error (SSE). This objective function was minimized using the expression [13]:

$$SSE = \sum_{i=1}^n (E^{exp.}(t_i) - E^{mod.}(t_i))^2 \quad (9)$$

where n is the number of experimental sample points, $E^{exp.}(t)$ is the experimental RTD data, and $E^{mod.}(t)$ is the simulated model RTD response.

Table 2 presents the effect of liquid flow rate on MRT and ADC of liquid. MRT decreased with the liquid flow rate due to increase in liquid velocity, but the liquid phase ADC increased. The values of vessel dispersion number at different liquid flow rate were calculated. It is observed that in an empty bed with increasing Reynolds number, N_D decreased and then increased. This decreasing and increasing in trend of N_D with Reynolds number was also observed by Biscoff (1962). In fixed bed regime, N_D decreased with increasing in liquid flow rate and had a minimum at the liquid flow rate of 80 cm³/s. The bed started to become fluidized at a liquid flow rate of 130 cm³/s, and vessel dispersion number (N_D) increased with increasing in liquid flow rate at this regime.

The ADC was varied between 4.63 and 12.47 cm²/s in the fixed

Table 1. Effect of liquid flow rate on pressure drop (Fixed and fluidized bed regime)

Bed regime	Q cm ³ /s	H cm	-	U _o cm/s	U _{act.} cm/s	Re _p -	ΔP ^{exp.} cmHg	ΔP ^{cal.*} cmHg
Fixed bed	34			1.73	6.44	43	3.5	2.47
	44	73	0.269	2.24	8.33	56	4.8	3.63
	80			4.08	15.15	102	13.4	9.41
	110			5.61	20.80	140	19.2	16.16
Fluidized bed	130	74	0.274	6.62	24.18	165	24.0	26.75
	170	76	0.293	8.66	29.55	216	32.8	33.52
	220	82	0.344	11.21	32.51	279	34.1	35.19

*Pressure drop was calculated by Foscolo et al. equation

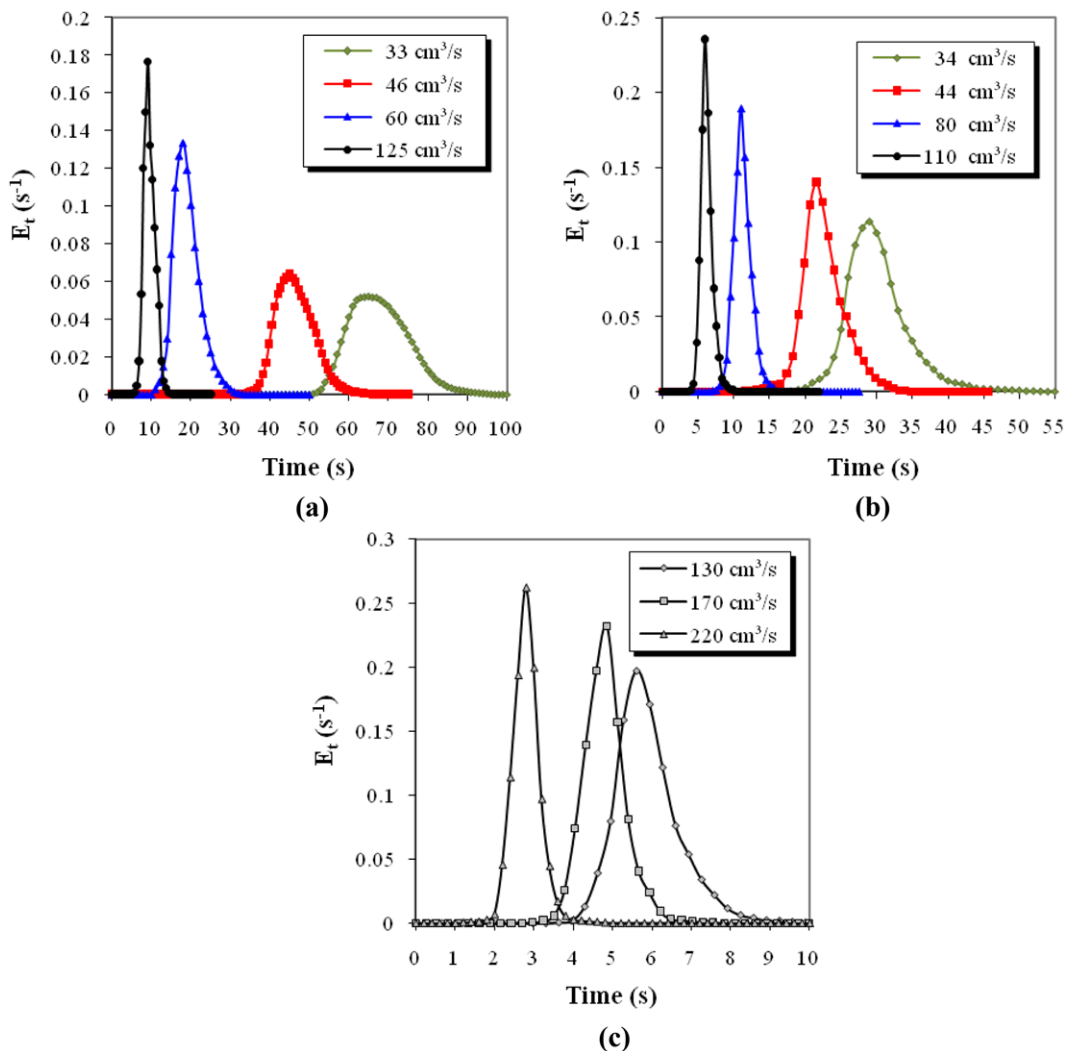


Fig. 2. RTD curves of liquid at different liquid flow rates (a) Empty bed (b) Fixed bed (c) Fluidized bed.

Table 2. Comparsion between experimental and model values of ADC, Pe and N_D (Ar=828113)

Bed regime	Q	Re_p	t_m	$D_1^{exp.}$	$Pe^{exp.}$	$N_D^{exp.}$	$D_1^{cal.}$	$Pe^{cal.}$	$N_D^{cal.}$
	cm^3	-	s	cm^2/s	-	-	cm^2/s	-	-
Empty bed	33	-	67.9	0.78	194	0.0057	0.95	159	0.0063
	46		46.4	1.01	200	0.0050	1.11	189	0.0053
	60		18.9	4.74	68	0.0147	3.62	76	0.0132
	125		9.5	6.04	95	0.0105	6.37	90	0.0111
Fixed bed	34	43	30.1	4.63	101	0.0093	5.09	92	0.0108
	44	56	22.2	5.14	118	0.0085	5.81	105	0.0095
	80	102	11.2	6.46	171	0.0058	8.41	131	0.0076
	110	140	6.2	12.47	122	0.0082	13.95	109	0.0092
Fluidized bed	130	165	5.9	14.95	146	0.0084	13.78	159	0.0077
	170	216	4.9	17.47	128	0.0078	15.51	145	0.0069
	220	279	2.8	20.70	129	0.0077	17.53	153	0.0066

bed regime and between 14.95 and 20.7 cm^2/s in the fluidized bed regime. With increasing the liquid superficial velocity, the variance of RTD curves decreases, and we expected that ADC decreases, whereas the calculated ADC shows the opposite meaning. It increases

with increasing the liquid superficial velocity, as also reported by Cho et al. [20] and Kim et al. [21]. On the other hand, the effect of liquid velocity, which was not considered in variance, was included in the ADC. Fig. 3 shows the influence of particle Reynolds num-

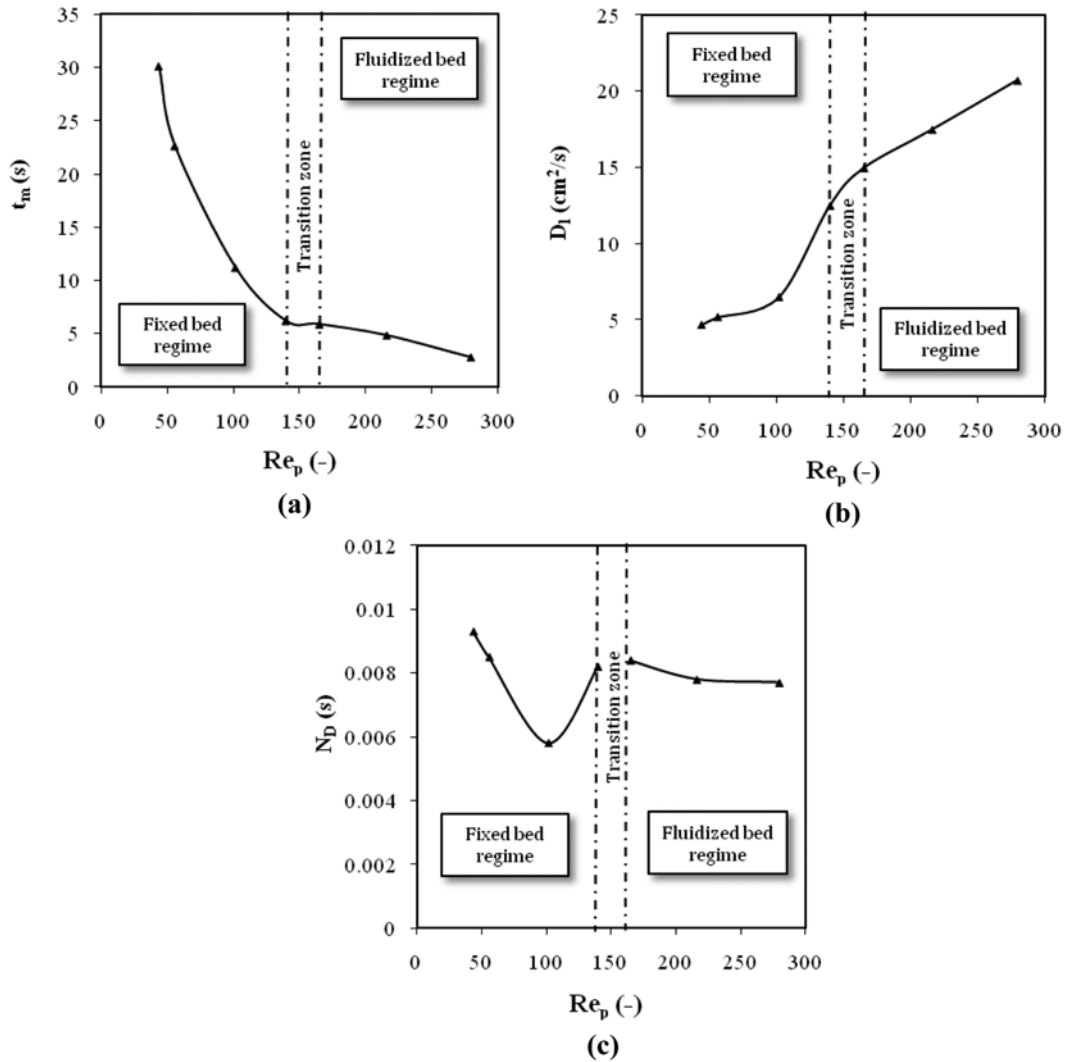


Fig. 3. Effect of particle Reynolds number on liquid phase mixing properties (a) Mean residence time (b) Axial dispersion coefficient (c) Vessel dispersion number.

ber on the mixing properties. Fig. 3(a) shows the mean residence time of the liquid phase (t_m) obtained from the RTD data. As particle Reynolds number increased, mean residence time decreased [20]. The variation in ADC of liquid phase with particle Reynolds number is shown in Fig. 3(b). The ADC increases with increasing Reynolds number. With increasing liquid velocity, the movement of particles intensifies, and thus the liquid in the bed is subjected to increasingly vigorous turbulence, resulting in the increase of mixing of the liquid phase [6]. The increase in axial dispersion coefficient with liquid velocity is also observed by Chung and Wen [9],

Tang and Fan [11], Krishnasamy and Shemilt [22] for classical liquid-solid fluidized bed. Also, the ADC in fixed bed regime is smaller than in the fluidized bed regime. Fig. 3(c) shows the vessel dispersion number (N_D) at different particle Reynolds numbers in fixed and fluidized bed regimes. In the fixed bed regime, it decreases with particle Reynolds number and then increases. In the fluidized bed regime, it decreases with increasing particle Reynolds number. Our experimental results have good agreement with the dispersion model with open-open boundary coefficient.

Table 3 shows ADC of liquid phase at different Re_p/Re_{mf} for par-

Table 3. ADC of liquid phase at different Re_p/Re_{mf} for particles diameter of 0.245 cm

Correlation	d_c	ρ_p	$ \rho_p - \rho_l $	Ar	Re_{mf}	$Re_p/Re_{mf}(D_l \text{ (cm}^2/\text{s)})$		
	cm	g/cm ³	g/cm ³	-	-	$Re_p:165$	$Re_p:216$	$Re_p:279$
Renganathan et al. (2004)	8.90	0.917	0.080	6806	3.9	42.4 (32.71)	55.5 (52.12)	71.6 (81.15)
		0.897	0.100	8508	4.8	34.3 (26.33)	44.9 (41.95)	58.03 (65.3)
Tang and Fan (1990)	7.62	1.180	0.183	15570	8.4	19.7 (14.99)	25.8 (23.90)	33.3 (37.21)
This work	5.00	10.730	9.730	828113	153.2	1.08 (13.78)	1.41 (15.51)	1.82 (1753)

ticles of 0.245 cm in diameter and different densities. Our experimental results were compared with that predicted by Tang and Fan (low density particles) and Renganathan and Krishnaiah (very low density particles) for the identical particle diameter of 0.245 cm. ADC increased with increase in liquid superficial velocity (Reynolds number), in our experimental range of flow rate. As the difference between solid and liquid density increases, ADC decreases in an identical Reynolds number. For high density particles, the ADC cannot be predicted certainly by existing published correlation equations, which are developed for beds of low density particles, indicating that particle density affects axial liquid mixing behavior significantly. Also, Chung and Wen demonstrated that ADC in a fluidized bed of low density particles behaves differently from a bed of heavy particles. ADC increases with increase Re_p/Re_{mf} in each constant Archimedes number. With increase in Archimedes number (Ar), the minimum fluidization velocity as well as minimum fluidization Reynolds number increases. Therefore, the actual liquid velocity is more for particles with a higher Archimedes number than for particles with a lower Archimedes number, which is also observed by Lee [4]. In the fluidized bed regime, increased liquid velocity implies more axial dispersion coefficient as explained under the effect of liquid velocity. This explains the reason for the increasing trend of axial dispersion coefficient with Archimedes number, which is also observed by Tang and Fan [8] and Chung and Wen [9] in classical liquid-solid fluidized beds. Literature studies on the liquid axial dispersion coefficients in liquid-solid fluidized beds show significant scatter. This scattering may be associated with the measuring techniques and specific system designs such as column size and distributor design. ADC of light particles is more than that of heavy particles in a constant particle Reynolds number and fluidized bed regime. The obtained experimental values for heavy density particles present the following relationships:

$$N_D = 10^{-6} Re_p^2 - 2 \times 10^{-4} Re_p + 1.76 \times 10^{-2} \quad \text{Fixed bed regime} \quad (10)$$

and

$$N_D = 9 \times 10^{-8} Re_p^2 - 5 \times 10^{-5} Re_p + 1.35 \times 10^{-2} \quad \text{Fluidized bed regime} \quad (11)$$

CONCLUSIONS

An experimental investigation of mixing characteristics and axial dispersion coefficient was performed in a liquid-solid bed of constant diameter. Results show that the axial dispersion coefficient (ADC) of a liquid increased with increasing particle Reynolds number and Archimedes number for heavy particles. It was observed that particle density affects axial liquid mixing behavior significantly. In a constant Reynolds number, the high density particles present less ADC than the low density particles. The ADC cannot be predicted precisely by Tang et al. and Renganathan et al. correlations, because these literature equations were obtained for light and very light particles. This is due to the fact that it is very sensitive to liquid interstitial velocity. Results have good agreement with the dispersion model (open-open boundary condition).

NOMENCLATURE

A : cross-sectional area of bed [cm²]

ADC	: axial dispersion coefficient [cm ² /s]
Ar	: archimedes number [-]
C	: concentration [mol/cm ³]
d _c	: diameter of column [cm]
d _p	: diameter of particle [cm]
D _l	: liquid phase axial dispersion coefficient [cm ² /s]
D _l ^{cal}	: calculated liquid phase axial dispersion coefficient [cm ² /s]
D _l ^{exp}	: experimental liquid phase axial dispersion coefficient [cm ² /s]
E ^{exp} (t _i)	: exit age distribution measured at sampling point [1/s]
E ^{mod} (t _i)	: exit age distribution predicted at sampling point [1/s]
E _t	: exit age distribution [1/s]
E _θ	: dimensionless exit age distribution [-]
g	: acceleration due to gravity [cm/s ²]
H	: bed height [cm]
L	: bed length [cm]
L _p	: length of cylindrical particle [cm]
n	: number of experimental sample points [-]
N _D	: vessel dispersion number [-]
N _D ^{cal}	: calculated vessel dispersion number [-]
N _D ^{exp}	: experimental vessel dispersion number [-]
Pe	: liquid phase Peclet number [-]
Pe ^{cal}	: calculated liquid phase Peclet number [-]
Pe ^{exp}	: experimental liquid phase Peclet number [-]
Q	: liquid flow rate [cm ³ /s]
Re _p	: particle Reynolds number [-]
Re _{mf}	: particle Reynolds number at minimum fluidization [-]
RTD	: residence time distribution [-]
SSE	: objective function [1/s ²]
t	: time [s]
t _m	: mean residence time of liquid obtained from RTD curve [s]
U _o	: superficial liquid velocity [cm/s]
U _{act}	: actual liquid velocity [cm/s]
U _{mf}	: minimum fluidization liquid velocity [cm/s]
x	: direction of flow [cm]
z	: dimensionless direction of flow [-]

Greek Letters

ΔP	: pressure drop [cmHg]
ΔP ^{cal}	: calculated pressure drop [cmHg]
ΔP ^{exp}	: experimental pressure drop [cmHg]
Δt	: the step time [s]
ε	: average void fraction of bed [-]
θ	: dimensionless residence time of liquid [-]
ρ _l	: liquid density [g/cm ³]
ρ _p	: particle density [g/cm ³]

Subscripts

l	: liquid
p	: particle

REFERENCES

1. B. G M. van Wachem and A. E. Almstedt, *Chem. Eng. J.*, **96**, 81 (2003).
2. M. Aghajani, H. Müller-Steinhagen and M. Jamialahmadi, *Int. J. Heat Mass Transfer*, **48**, 317 (2005).
3. S. Limtrakul, J. Chen, P. A. Ramachandran and M. P. Dudukoviæ,

Chem. Eng. Sci., **60**, 1889 (2005).

4. D. H. Lee, *Korean J. Chem. Eng.*, **18**, 347 (2001).
5. G. Jin and D. Liu, *Powder Technol.*, **154**, 138 (2005).
6. T. Renganathan and K. Krishnaiah, *Chem. Eng. J.*, **98**, 213 (2004).
7. M. Asif, N. Kalogerakis and L. Behie, *Chem. Eng. Sci.*, **47**, 4155 (1992).
8. W. T. Tang and L. S. Fan, *Chem. Eng. Sci.*, **45**, 543 (1990).
9. S. F. Chung and C. Y. Wen, *AICHE J.*, **14**, 857 (1968).
10. K. I. Kikuchi, H. Konno, S. Kakutani, T. Sugawara and H. Ohashi, *J. Chem. Eng. Japan*, **19**, 362 (1984).
11. W. T. Tang and L. S. Fan, *AICHE J.*, **35**, 355 (1989).
12. O. Levenspiel, *Chem. React. Eng.*, 3rd Ed., John Wiley & Sons, New York, 668 (1999).
13. O. Levenspiel and W. K. Smith, *Chem. Eng. Sci.*, **6**, 227 (1957).
14. D. Kunii and O. Levenspiel, *Fluidization Eng.*, 2nd Ed., Butterworth-Heinemann, Boston, 491 (1991).
15. V. L. Streeter, E. B. Wylie and K. W. Bedford, *Fluid mechanics*, 9th Ed. McGraw-Hill, New York, 740 (1998).
16. E. van Zessen, Hydrodynamics of liquid-liquid-solid fluidized bed bioreactor, *Ph.D Thesis*, Wageningen University, Netherland, 200 (2003).
17. H. M. Jena, G. K. Roy and B. C. Meikap, *Powder Technol.*, **196**, 246 (2009).
18. S. J. Kim, S. Y. Jeung and H. Moon, *Korean J. Chem. Eng.*, **15**, 637 (1998).
19. J. F. Richardson and W. N. Zaki, *Trans. Inst. Chem. Eng.*, **32**, 35 (1954).
20. H. I. Cho, C. H. Chung, G. Y. Han, G. R. Ahn and J. S. Kong, *Korean J. Chem. Eng.*, **17**, 292 (2000).
21. J. Kim, G. Han and C. Yi, *Korean J. Chem. Eng.*, **19**, 491 (2002).
22. P. R. Krishnaswamy and L. W. Shemilt, *Can. J. Chem. Eng.*, **51**, 680 (1973).